



**HAL**  
open science

## Role of the TMG flow rate on the GaN layer properties grown by MOVPE on (hkl) GaAs substrates

J. Laifi, C. Saidi, N. Chaaben, A. Bchetnia, Y. El Gmili, Jean-Paul Salvestrini

### ► To cite this version:

J. Laifi, C. Saidi, N. Chaaben, A. Bchetnia, Y. El Gmili, et al.. Role of the TMG flow rate on the GaN layer properties grown by MOVPE on (hkl) GaAs substrates. *Materials Science in Semiconductor Processing*, 2019, 101, pp.253-261. 10.1016/j.mssp.2019.06.006 . hal-02282621

**HAL Id: hal-02282621**

**<https://hal.science/hal-02282621>**

Submitted on 24 Feb 2023

**HAL** is a multi-disciplinary open access archive for the deposit and dissemination of scientific research documents, whether they are published or not. The documents may come from teaching and research institutions in France or abroad, or from public or private research centers.

L'archive ouverte pluridisciplinaire **HAL**, est destinée au dépôt et à la diffusion de documents scientifiques de niveau recherche, publiés ou non, émanant des établissements d'enseignement et de recherche français ou étrangers, des laboratoires publics ou privés.



Distributed under a Creative Commons Attribution - NonCommercial 4.0 International License

# Role of the TMG flow rate on the GaN layer properties grown by MOVPE on (hkl) GaAs substrates

J. Laifi<sup>a,b,\*</sup>, C. Saidi<sup>a</sup>, N. Chaaben<sup>a</sup>, A. Bchetnia<sup>a,d</sup>, Y. El Gmili<sup>c</sup>, J.P. Salvestrini<sup>c</sup>

<sup>a</sup> *Unité de Recherche sur les Hétéro-Epitaxies et Applications, Faculté des Sciences de Monastir 5019, Université de Monastir, Tunisia*

<sup>b</sup> *Physics Department, College of Science, Jouf University, P.O. Box: 2014, Sakaka, Saudi Arabia*

<sup>c</sup> *CNRS, UMI 2958 Georgia Tech-CNRS, 57070, Metz, France*

<sup>d</sup> *Department of Physics, College of Science, Qassim University, Saudi Arabia*

The role of the TMG flow rate on the properties of the GaN layer grown by MOVPE on (001) and (11n)/n = 2,3 GaAs substrates were investigated. The surface morphology, crystalline quality and optical property were found to be strongly dependent on the TMG flow rate. As the latter decreased to 16  $\mu\text{mol}/\text{min}$ , in-situ reflectance measurements showed a constant signal. This is attributed to the enhanced coalescence process, which resulted in the improvement of the surface morphology. A high TMG flow rate of 40  $\mu\text{mol}/\text{min}$  sccm promoted predominantly vertical growth and resulted in the formation of a three-dimensional island. The lowest YL intensity and FWHM values of near band edge emission were obtained for GaN layers grown on (001) GaAs substrate with a TMG flow rate of 16  $\mu\text{mol}/\text{min}$ , indicating an improvement of the optical properties of the GaN layer. This improvement is attributed to the coalescence process at the initial growth stage of GaN and the lateral growth process. All these behaviors were always observable whatever the used substrates. Depth resolved-CL showed that a mechanism of phase transformation in response to changing the substrate orientations.

## 1. Introduction

III-V semiconductor compounds have emerged as new promising materials for applications in light-emitting diodes (LEDs), laser diodes (LDs) and high electron mobility transistors (HEMTs) [1–3]. Particularly, GaN is believed to be suitable to high power and in high frequency devices due to their interesting physical and chemical properties such as high melting point temperature, breakdown voltage and wider band gap.

Because bulk GaN crystals are not commercially available, GaN-based devices are mainly grown on sapphire and SiC substrates which are rather costly, thus affecting the device fabrication. In order to cut down their manufacturing costs, GaAs substrates have been employed as a promising alternative for the growth of GaN materials. GaN/GaAs structures are very attractive for the possibility they offer to grow cubic GaN layers and thus achieve more efficient light-emitting diodes [4–6]. Indeed, as opposed to hexagonal GaN, cubic GaN is free of piezoelectric field that appears in strained hexagonal structures and decreases the luminescence efficiency [7]. In addition, it was reported by Nakamura et al. [8] that the cubic phase of GaN may be more suitable to p-type doping than hexagonal GaN.

Nevertheless, the growth of GaN/GaAs structures is challenging because of the instability of GaAs substrate at high growth temperatures ( $> 600^\circ\text{C}$ ), and spontaneous phenomena such as etching of the GaAs by the nitrogen plasma and the diffusion of nitrogen or melting of Ga into the GaAs substrate [9]. Another issue is the lattice mismatch between GaN and GaAs ( $\approx 20\%$ ) leading to high density of stacking faults and dislocations ( $\approx 4.10^{12} \text{ cm}^{-2}$ ) in the epitaxial layers [10,11]. Nonetheless, the use of a homogenous or gradual GaN buffer layer prevents the degradation of the GaAs surface during the active layer growth at high temperature. In our previous study, we reported a critical thickness of 100 nm that allows maintaining the thermal stability and reaching good quality of GaN/GaAs structures [12]. In addition to a smooth GaN surface and flat GaN/GaAs interface, several growth conditions must be adequately controlled.

The studies conducted on this research issue are still limited to the use of (001) and (111) GaAs orientations as a substrate of GaN materials. Furthermore, the growth of GaN on high-index GaAs substrates may lead to the improvement of the physical properties of the layers compared to materials grown conventionally on (001) GaAs orientation. Interest in the use of (11n) GaAs substrate to grow semiconductor materials is diverse. Sonoprim et al. [13] found that the (113) GaAs

\* Corresponding author. Unité de Recherche sur les Hétéro-Epitaxies et Applications, Faculté des Sciences de Monastir 5019, Université de Monastir, Tunisia.,  
E-mail addresses: [jihed88laifi@yahoo.fr](mailto:jihed88laifi@yahoo.fr), [jlaifi@ju.edu.sa](mailto:jlaifi@ju.edu.sa) (J. Laifi).

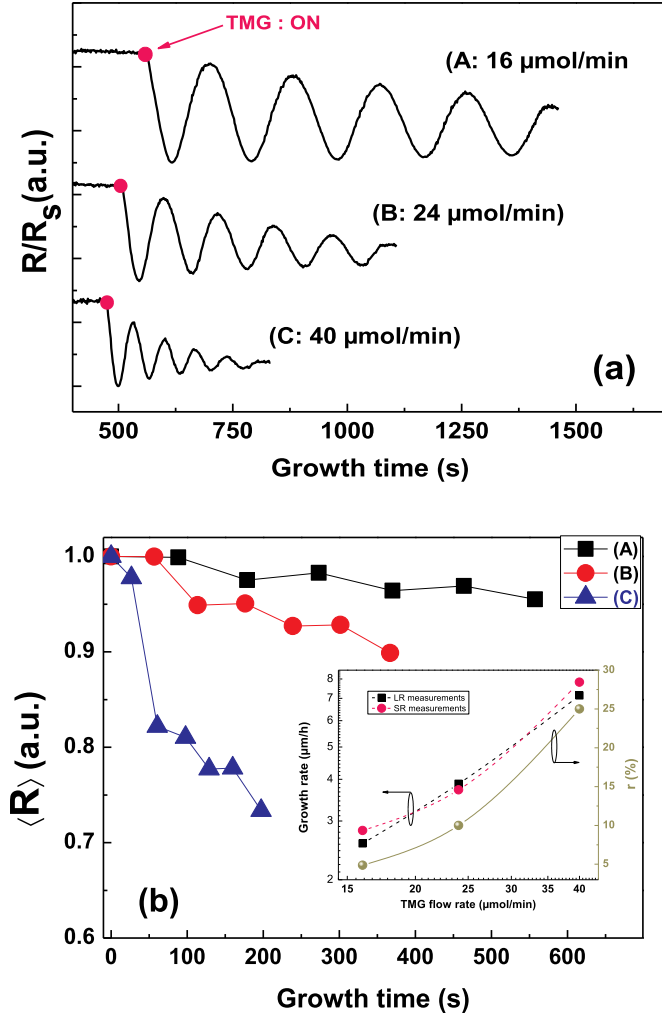


**Fig. 1.** (a) In-situ real time laser reflectometry signal recorded during the growth of GaN on GaAs (001) substrate. From run to run, the TMG flow rate was varied from 16 to 40  $\mu\text{mol}/\text{min}$ . Filled circle indicates the switching on of TMG into the reactor. (b) Reflectivity oscillations average value  $\langle R \rangle$  of GaN layers as a function of growth time for different TMG flow rates. Inset shows the plot of the relative reduction of  $\langle R \rangle$  ( $r$  %) and the growth rate versus TMG flow rate.

substrate is a promising substrate to grow GaN in cubic phase. In the study of Makimoto et al. [14], a smooth surface covered with small GaN grains was observed for the growth on (11 $\bar{1}$ )  $n = 3,5$  GaAs surface. The originality of the present work lies in the use of high index GaAs substrates oriented to (11 $\bar{1}$ )  $n = 2,3$  as well as the (001) orientation in order to better understand the growth mechanisms and to propose new alternatives to overcome the lack of substrates for GaN materials. In our previous study, we investigated the substrate orientation effects on the quality of the overgrown GaN layers. Our results showed that both (111) and (112) GaAs substrate orientations and high growth temperature ( $> 850^\circ\text{C}$ ) favor the hexagonal phase, whereas the cubic GaN phase was obtained on (001) and (113) GaAs substrates at low growth temperatures [15,16].

Nevertheless, the improvement of the GaN layer properties still needs further effort. In this paper, we report for the first time on the impact of TMG flow rate on the crystal quality of GaN films grown on (001) and (11 $\bar{1}$ )/ $n=2,3$  GaAs substrates at growth temperature of  $800^\circ\text{C}$ . The growth was monitored *in-situ* using laser reflectometry (LR), and the different layers were characterized using scanning electron

microscopy (SEM), atomic force microscopy (AFM), high resolution x-ray diffraction (HRXRD) and depth-resolved cathodoluminescence (CL).

## 2. Experiment details

GaN films were grown on (001) and (11 $\bar{1}$ )/ $n=2,3$  semi-insulating GaAs substrates in an atmospheric pressure MOVPE system (AP-MOVPE) using hydrogen ( $\text{H}_2$ ) carrier gas with a total flow rate of 2 slm (standard liters per minute). The different GaAs substrates were chemically cleaned and mounted simultaneously on a graphite susceptor and loaded into a vertical quartz reactor. The (hkl) GaAs substrates were first annealed in an atmosphere of  $\text{H}_2$  to remove the surface oxide. This step was followed by surface nitridation in which all substrates were exposed to 2 slm of ammonia ( $\text{NH}_3$ ) for 10 min at  $550^\circ\text{C}$ . Then, trimethylgallium (TMG =  $16 \mu\text{mol}/\text{min}$ ) and  $\text{NH}_3$  were supplied to grow 130 nm thick-GaN buffer layers at a growth temperature of  $550^\circ\text{C}$ . After that, the GaN layers were grown at a fixed growth temperature of  $800^\circ\text{C}$  with TMG flow rate ranging from  $16 \mu\text{mol}/\text{min}$  to  $40 \mu\text{mol}/\text{min}$ . At this growth level, the thicknesses of GaN layers were typically  $0.6 \mu\text{m}$ . The growth temperature of  $800^\circ\text{C}$  was found to improve the cubic phase structure of GaN samples. Indeed, we reported in our previous studies that high growth temperature ( $> 800^\circ\text{C}$ ) favor the GaN growth with hexagonal structure, whereas the GaN cubic structure was favored at low temperature [15]. The samples were characterized *in-situ* by Laser reflectometry (LR) and *ex-situ* by scanning electron microscopy (SEM), atomic force microscopy (AFM), high resolution x-ray diffraction (HRXRD) and depth-resolved cathodoluminescence (CL). Details of the characterization techniques were presented elsewhere [17].

## 3. Results and discussion

Laser reflectometry is the most common technique in MOVPE machines. It has been successfully used for real-time determination of growth rate, layer thickness, optical constants and surface morphology evolution during the growth [18,19]. Fig. 1 (a) shows the time dependence of the LR signal during the growth of GaN layers on GaAs (001) substrate at  $800^\circ\text{C}$  for a TMG flow rate ranging from 16 to 40  $\mu\text{mol}/\text{min}$ . The increase of TMG flow rate affected the reflectivity oscillations average value  $\langle R \rangle$  defined by [20]:

$$\langle R \rangle = \left( \frac{R_{i-\max} + R_{i-\min}}{2} \right) \quad (1)$$

where  $R_{i-\max}$  and  $R_{i-\min}$  are the maximum and minimum of the reflectivity oscillations, respectively. The variations of  $\langle R \rangle$  versus the growth time for different TMG flow rates are plotted in Fig. 1 (b). For the growth with a TMG flow rate of  $16 \mu\text{mol}/\text{min}$  (sample A),  $\langle R \rangle$  kept a virtually constant value, which clearly indicates a smoother GaN surface morphology. As the TMG flow rate was increased (sample B), the *in-situ* reflectance signal showed a decrease of the reflectivity oscillations average value  $\langle R \rangle$ .

The relative reduction  $r$  of  $\langle R \rangle$ , defined as  $r(\%) = \left( \frac{\langle R \rangle_{\text{First}} + \langle R \rangle_{\text{Last}}}{R_{\text{First}}} \right) \times 100$ , where  $\langle R \rangle_{\text{First}}$  and  $\langle R \rangle_{\text{Last}}$  are, respectively, the first and last average values, is plotted in the inset of Fig. 1 (b) with respect to the TMG flow rate. The value of  $r$  increases with the increase of the TMG flow rate. For sample C, grown with the highest TMG flow rate, the  $\langle R \rangle$  value was reduced by 25%. This behavior is attributed to the reflected signal diffusion caused by the rough surface morphology and the larger island size in the initial stage of growth [21]. The increase of TMG flow rate resulted in the enhancement of the vertical growth rate value ( $V_R$ ) and corresponds to a 3D-growth mode. As shown in the inset of Fig. 1 (b), the growth rate follows the TMG flow rate.  $V_R$  is calculated from the reflectivity oscillations by using the following equation [22]:

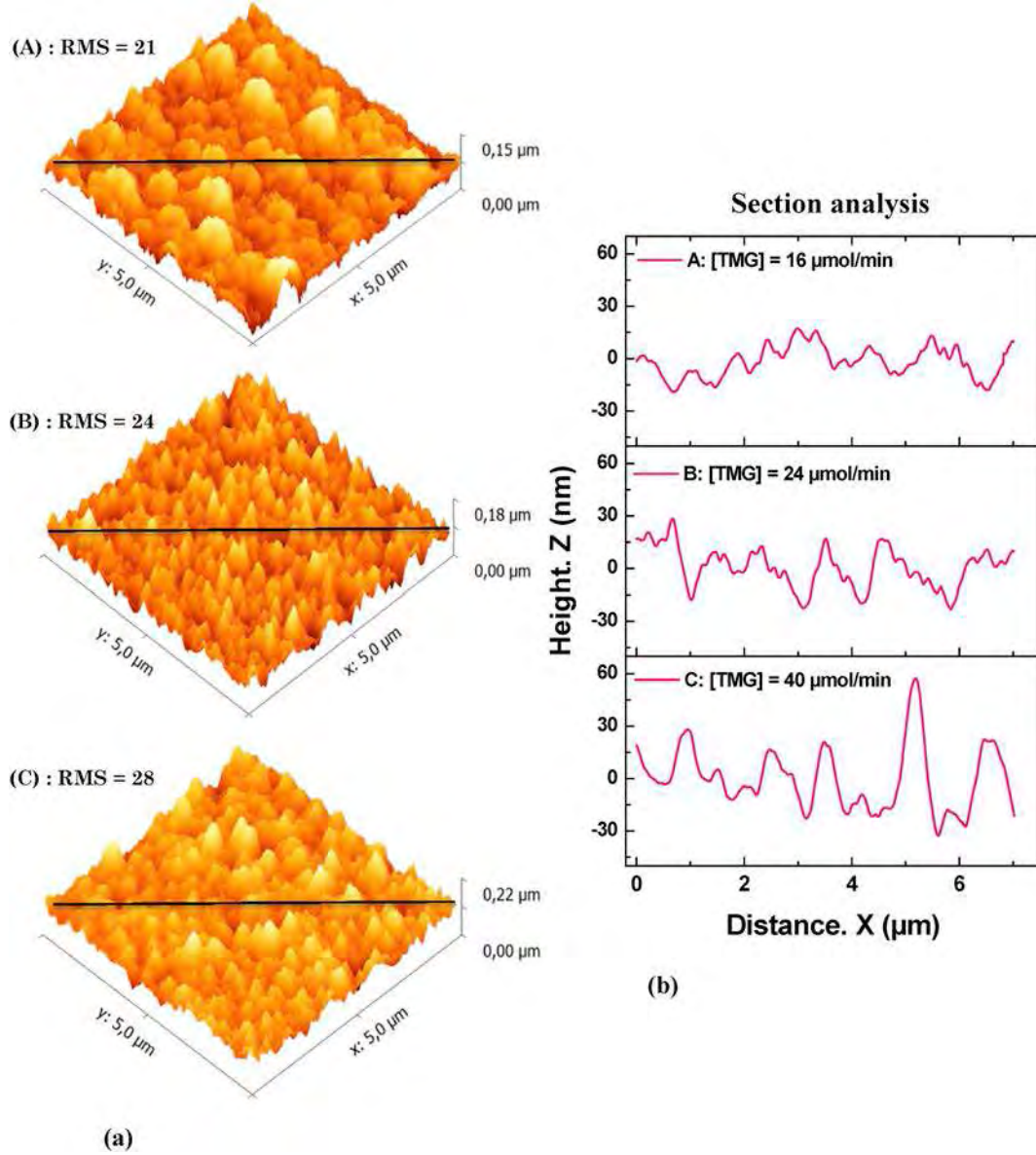


**Fig. 2.** (a) AFM images of GaN layers grown on GaAs (001) substrates with TMG flow rates of 16  $\mu\text{mol}/\text{min}$  (A), 24  $\mu\text{mol}/\text{min}$  (B) and 40  $\mu\text{mol}/\text{min}$  (C). (b) Cross section profile of the three samples.

$$V_R = \frac{\lambda}{2nT} \quad (2)$$

where  $\lambda$ ,  $n$  and  $T$  are, respectively, the wavelength of the incident laser beam, the refractive index of GaN layer and the reflectivity oscillations period. For more accuracy, in the inset of Fig. 1 (b), we added the growth rate values of GaN layers extracted from multi-wave reflectance measurements (SR). As clearly displayed, the results of SR measurements are in good accordance with the LR results.

In Fig. 2 (a), further assessment of the surface morphology of the samples, shows the AFM images of the sample surfaces grown with TMG flow rates of 16, 24 and 40  $\mu\text{mol}/\text{min}$ , respectively. With a low TMG flow rate (sample A), a wavy surface with coalesced small islands is observed. At higher TMG flow rates (samples B and C), the sizes and densities of islands increased. Fig. 2 (b) shows the profiles of the AFM

image cross section taken along the lines shown in Fig. 2 (a). They show that islands in sample A grown with a low TMG flow rate exhibit a quasi-rounded shape distribution with an RMS value of 21 nm; whereas, for a higher TMG flow rate, the profiles show a quasi-triangular distribution of islands with an RMS value of 24 nm and 28 nm for samples B and C, respectively. The origin of the rough surface morphologies correlates with the enhanced Ga supply rate at a high TMG flow rate. Thus, GaN islands having a small size tend to coalesce into bigger ones, due to the excess of Ga migrating on the surface [23,24]. This coalescence enables the decrease of GaN island density. 2D-like growth of GaN is thus favored using low TMG flow rates even if N atoms do not react, because of a lack of Ga atoms, leading to a wavy surface.

To further understand this behavior, we analyzed the surface morphology of the GaN layers grown on substrates with different orientations and with different TMG flow rates. The corresponding SEM images

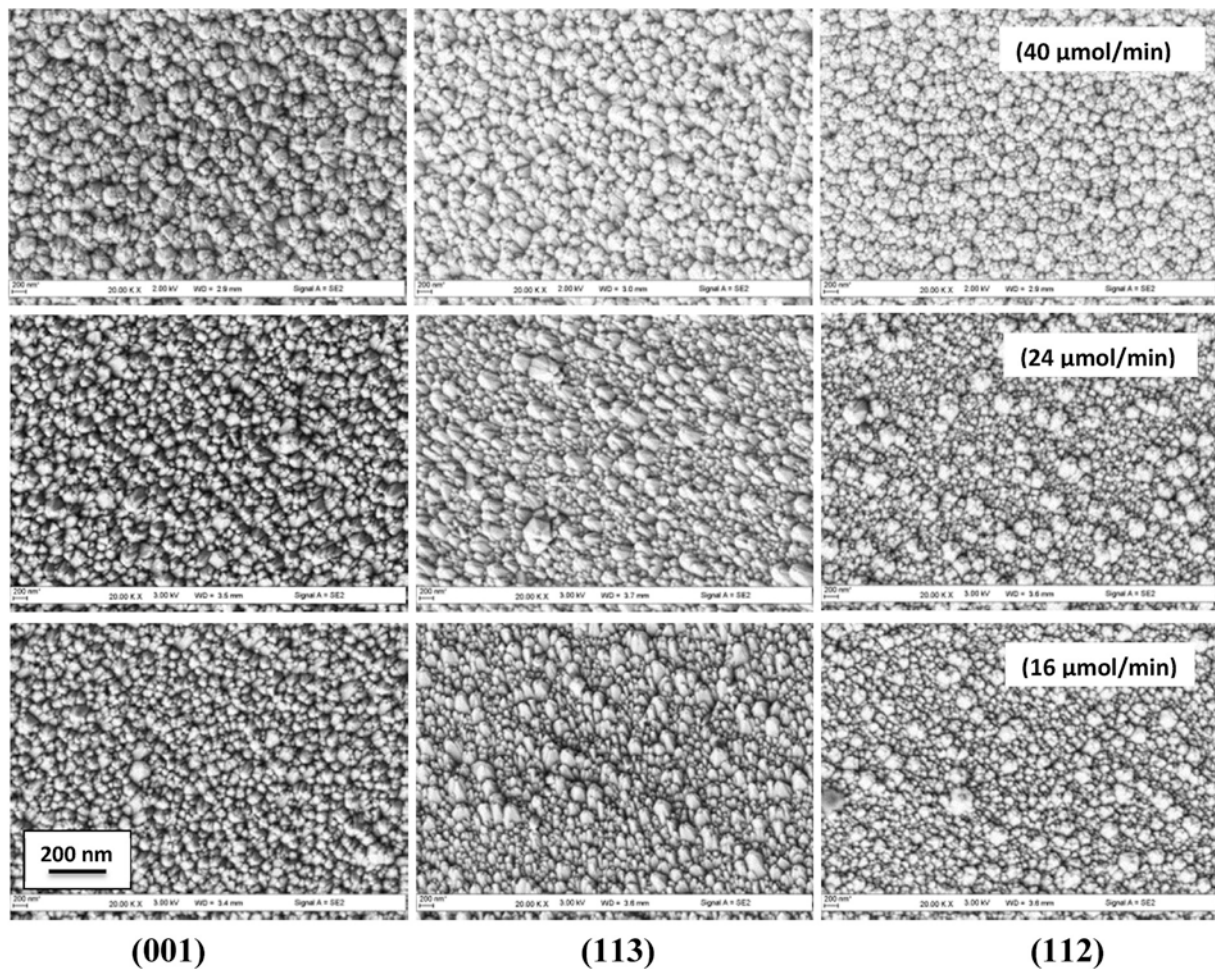


**Fig. 3.** SEM images indicating the surface morphologies of GaN layers grown on different orientations of GaAs substrate with TMG flow rates of 16  $\mu\text{mol}/\text{min}$ , 24  $\mu\text{mol}/\text{min}$  and 40  $\mu\text{mol}/\text{min}$ .

are reported in Fig. 3. All the samples exhibited three dimensional island structures whatever the substrate orientation and flow rates. As shown previously, low TMG flow rates lead to the formation of GaN islands with small diameter and height. This is evidenced in Fig. 4 (a) which shows the island size distribution in a GaN layer grown on a (001) GaAs substrate and for different TMG flow rates. The increase of the TMG flow rate strongly increased the average island size from 118 nm to 198 nm. The same trend is observed in the GaN layers grown on substrates with different orientations. This behavior was accompanied by an increase of the RMS (deduced from AFM measurements), from 13 to 30 nm and 16–35 nm for the growth on (113) and (112) GaAs substrate orientations, respectively.

The substrate orientation also plays a role in the morphology of the GaN layers (see Fig. 3). For a TMG flow rate of 16  $\mu\text{mol}/\text{min}$ , the GaN layer grown on (001) GaAs substrate consisted of closely packed GaN islands with an average size of about 118 nm (see Fig. 4 (b)). The growth on (113) GaAs substrate revealed islands with an elongated form with a top acute apex. Their average size was about 200 nm. The surface morphology of the GaN layer grown on GaAs (112) substrate indicated the presence of some islands with hexagonal shape and distributed over the surface. Their typical average size as deduced from Fig. 4 (b) was about 245 nm.

As regards the crystalline quality of our GaN layers, Fig. 5(A)–(C) shows the XRD diffraction pattern of the GaN/GaAs (hkl) samples

deposited with a TMG flow rate of 16  $\mu\text{mol}/\text{min}$ . For growth on (001) GaAs substrate (Fig. 5 (A)), we noted the presence of a peak at  $40.01^\circ$  corresponding to the plane (200) of the cubic crystalline phase (c-GaN). Intensity of the peak at  $34.51^\circ$  was related to the hexagonal (002) and the cubic (111) plans. Other peaks located at  $31.70^\circ$  and  $66.20^\circ$  are assigned to (002) and (004) planes of the GaAs substrate. By changing the substrate orientation to (113) (figure (B)), we clearly noticed, in addition to the peak corresponding to the (113) plane of GaAs substrate located at  $53.54^\circ$ , the presence of a broad peak at  $68.82^\circ$ . The latter is an overlap of peaks related to h-GaN and c-GaN phases. By dividing the XRD-intensity as seen in the inset of Fig. 5, we observed peaks located at  $65.03^\circ$  and  $68.98^\circ$  related to the (103) and (113) planes of h-GaN and c-GaN, respectively. The peak located at  $78.88^\circ$  corresponds to the (202) plane of h-GaN. The XRD spectrum of the GaN sample grown on (112) GaAs substrate, illustrated by Fig. 5 (C), shows the presence of peaks located at  $38.21^\circ$ ,  $44.27^\circ$ ,  $64.77^\circ$  and  $78.88^\circ$  assigned respectively to (101), (102), (103) and (202) of h-GaN planes. The obtained XRD peaks positions were very similar to the results reported by Gastellou et al. [25]. All the output parameters from Fig. 5 are summarized in Table 1. By comparing the FWHMs of cubic and hexagonal diffraction peaks, we note that the highest values were obtained for cubic GaN peaks, which indicates the alignment of the GaN layers with respect to  $\langle 00.1 \rangle$  axis of the wurtzite structure. The substrate orientation dependence of the GaN layer properties could be related to the surface

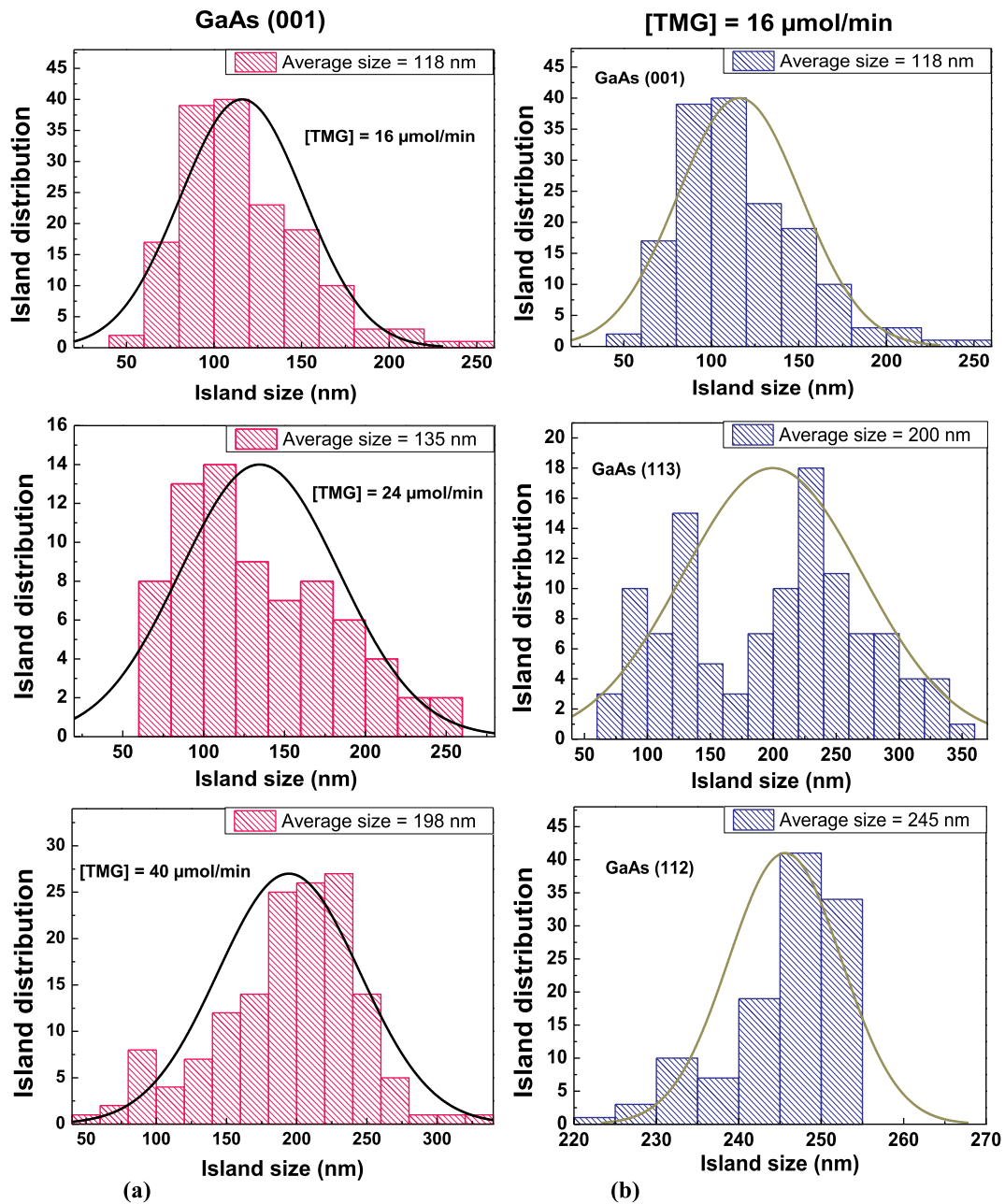


Fig. 4. (a) Pattern histograms of GaN layer grown on (001) GaAs substrate with TMG flow rate ranging from 16 to 40  $\mu\text{mol}/\text{min}$  (pink filled pattern histograms). (b) Pattern histograms of GaN layer grown on different GaAs orientations for TMG flow rate of 16  $\mu\text{mol}/\text{min}$  (blue filled pattern histograms). (For interpretation of the references to colour in this figure legend, the reader is referred to the Web version of this article.)

structure of the (hkl) GaAs substrates [26,27]. The microscopic surface of (001) GaAs substrate is composed of atoms with unsaturated bonds called dimers oriented along the  $[-110]$  direction for arsenic atoms and  $[110]$  for gallium atoms. (11 $\bar{n}$ ) GaAs surfaces had a mixed nature due to the existence of both single and double dangling bonds. Thus, during the growth process, an incident N atom must form one bond with the Ga atoms in the case of (11 $\bar{n}$ ) GaAs substrate, while it has to form two bonds in the case of (001) GaAs substrate. Thus, for the (11 $\bar{n}$ ) orientations the probability of desorbing an N atom is greater since it is less bound. In addition, the generation of (001) plane terraces terminated by (111) step edges [15] could favor the incorporation of species.

All of this could explain the different GaN layer morphologies obtained on the different GaAs substrates.

Fig. 6 (a)-(c) illustrates the room-temperature cathodoluminescence (CL) spectra of GaN layers grown on (001), (113) and (112) oriented GaAs substrates with TMG flow rate of 16 and 24  $\mu\text{mol}/\text{min}$ . No CL emission was observed in the samples grown with a TMG flow rate of 40  $\mu\text{mol}/\text{min}$ . In all spectra, we note the presence of a broad deep level emission at 2.4 eV corresponding to the yellow band luminescence (YB) and sharp near-band-edge emission (NBE) peaks at 3.21 eV which is attributed to the cubic phase of GaN [17]. The latter was dominant in the samples grown with TMG = 16  $\mu\text{mol}/\text{min}$ , as reported in Fig. 6 (d). The comparison of the

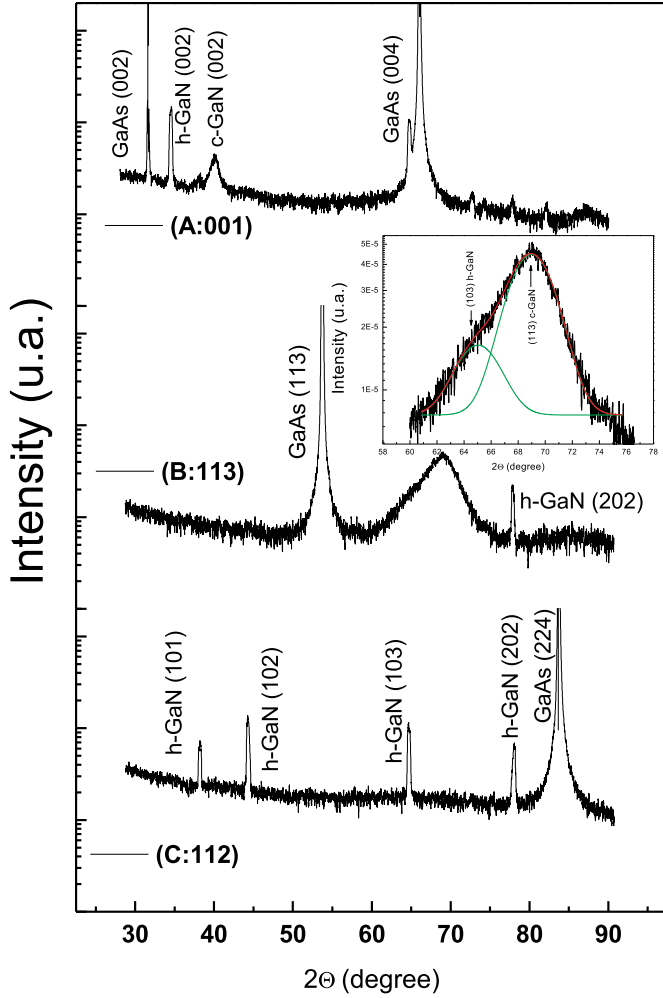


Fig. 5. XRD patterns of the GaN samples deposited on (A) (001), (B) (113) and (C) (112) GaAs substrates with TMG flow rate of 16  $\mu\text{mol}/\text{min}$ . The inset is a zoom of peak observed for growth of GaN on GaAs (113).

Table 1

Output parameters (peak position, FWHM and peak intensity) of x-ray diffraction. The values of each parameter are given with the same number of significant digits.

Substrate orientation	(hkl) Peak diffraction	Peak position ( $^{\circ}$ )	FWHM ( $^{\circ}$ )	Peak intensity (counts/s)
(001) GaAs	h-GaN (002)/c-GaN (111)	34.51	0.349	173.21
	c-GaN (002)	40.01	1.267	27.81
(113) GaAs	h-GaN (103)	65.03	3.767	12.76
	c-GaN (113)	68.98	3.981	53.64
	h-GaN (202)	78.88	0.324	24.57
(112) GaAs	h-GaN (101)	38.21	0.327	43.85
	h-GaN (102)	44.27	0.353	101.81
	h-GaN (103)	64.77	0.356	85.12
	h-GaN (202)	78.88	0.384	45.36

full width at half maximum (FWHM) of NBE emission for all samples is shown in Fig. 6 (d). The highest value of FWHM was obtained for GaN layers grown on (113) GaAs substrate. This is the synonym of the presence of a larger density of defects in the GaN layer. This can be associated with the surface structure of (113) GaAs substrates exhibiting a high step density, which favor the presence of the stacking faults (SFs) [15,28]. In Fig. 6 (d), the yellow intensity increases with the increase of TMG flow

rate in the GaN layers, whatever the used substrate orientation. First principle calculations predict that several  $V_{\text{Ga}}$ -related defects may be responsible for YL in undoped GaN [29]. On the other hand, Ogino and Aoki [30]. reported that Si and O doping do not affect the relative YL intensity while doping with carbon enhanced this emission. They associated the YL band to a complex involving a Ga vacancy and a C atom substituted for the nearest neighbour of the Ga sites. This same YL assignment was also suggested by other experimental groups [31–36]. In HVPE-grown GaN, Oh et al. [37] reported that by increasing the V/III ratio, the YL intensity decreases. They associated the YL extinction to the enhancement of the Ga vacancy concentration in correlation with the increase of the FWHM of the XRD (00.2) peak. The YL intensity diminution has also been shown in MOVPE-grown GaN by increasing the V/III ratio [38,39]. In our case, for the different substrate orientations, the FWHM has almost the same value for the different TMG flow rates synonym of a constant defects amount. Thus, we suggest that the Fig. 1, 2, 3, 4, 5, 6 and 7 increase of the TMG flow rate, which is accompanied by the rise of the C amount incorporated in GaN, is responsible for the YL intensity increase.

The lowest ratio and FWHM values were obtained for GaN layers grown on (001) GaAs substrate with a TMG flow rate of 16  $\mu\text{mol}/\text{min}$ , indicating an improvement of the optical properties of the GaN layer. Our results are consistent with those reported by Li et al. [40]. The TMG flow rate of 16  $\mu\text{mol}/\text{min}$  was selected for this purpose and used for the experiments discussed below.

The CL technique has the advantage of obtaining information resolved in depth via an increase of beam energy. Fig. 7 (a)-(c) describes the large area room-temperature depth resolved CL spectra recorded in the GaN/65 nm-GaN-BL samples grown on (hkl) GaAs substrates for electron beam energy of 5, 10, 15 and 20 keV. It is worth noting that all CL spectra reveal cubic GaN (c-GaN) NBE-emission located at 3.2 eV and no significant luminescence band corresponding to the hexagonal phase of GaN (3.4 eV). This result does not prove that our GaN samples are in purely cubic phase due to the small difference between the energy of formation of the two phases. The peak located at 3.2 eV is an overlap of broad peaks of the transitions in cubic GaN and some excitonic recombination in hexagonal GaN. All experimental data presented in Fig. 7 (a)-(c) can be fitted by a sum of two Gaussian functions centered at 3.16 eV and 3.27 eV. The first peak at 3.16 eV corresponds to the DA pair transition in cubic GaN [41], whereas the second peak is an overlap of broad peaks of the excitonic recombinations in cubic GaN and some transitions correlated to the transitions in hexagonal GaN [42]. In Fig. 7 (d), we plotted the energy position of c-GaN and h-GaN peaks as a function of the electron beam energy (deduced from the data of Fig. 7 (a)-(c)) for samples grown on (hkl) GaAs substrates. Contrary to the results obtained for growth on (001) and (112) substrate orientations, for which only a red shift of two peaks is observed, red and blue shifts of NBE peaks are seen for growth on (113) GaAs substrate. This behavior has been depicted by several authors, who attributed it to the local overheating induced by the electron beam and/or internal absorption effects [43–45]. But the shrinkage of band energy caused by heating of the surface during CL measurements would not exceed 5 meV [46]. Thus, the contribution of this effect in the energy red-shift of NBE-peaks observed in this work can be ruled out. In view of our measurements, we correlated the above behavior to the internal absorption effects. It is expected that the absorption spectrum across BE would cut the signal on the high energy side of the NBE excitonic emission and lead to the peak red shift with increasing beam energy.

The blue-shifts observed for the c-GaN and h-GaN BE-emission in the layer grown on the (113) GaAs substrate can be attributed to the increase of the energy gap induced by the strain effects [47]. This behavior is an indication of the increase of internal strains and the formation of a large number of stacking faults (SFs) for the growth of GaN on GaAs (113) substrate.

The above results indicate that our samples contain a mixture of cubic and hexagonal fractions of GaN crystals. In order to draw more information about the change of both phases as a function of growth

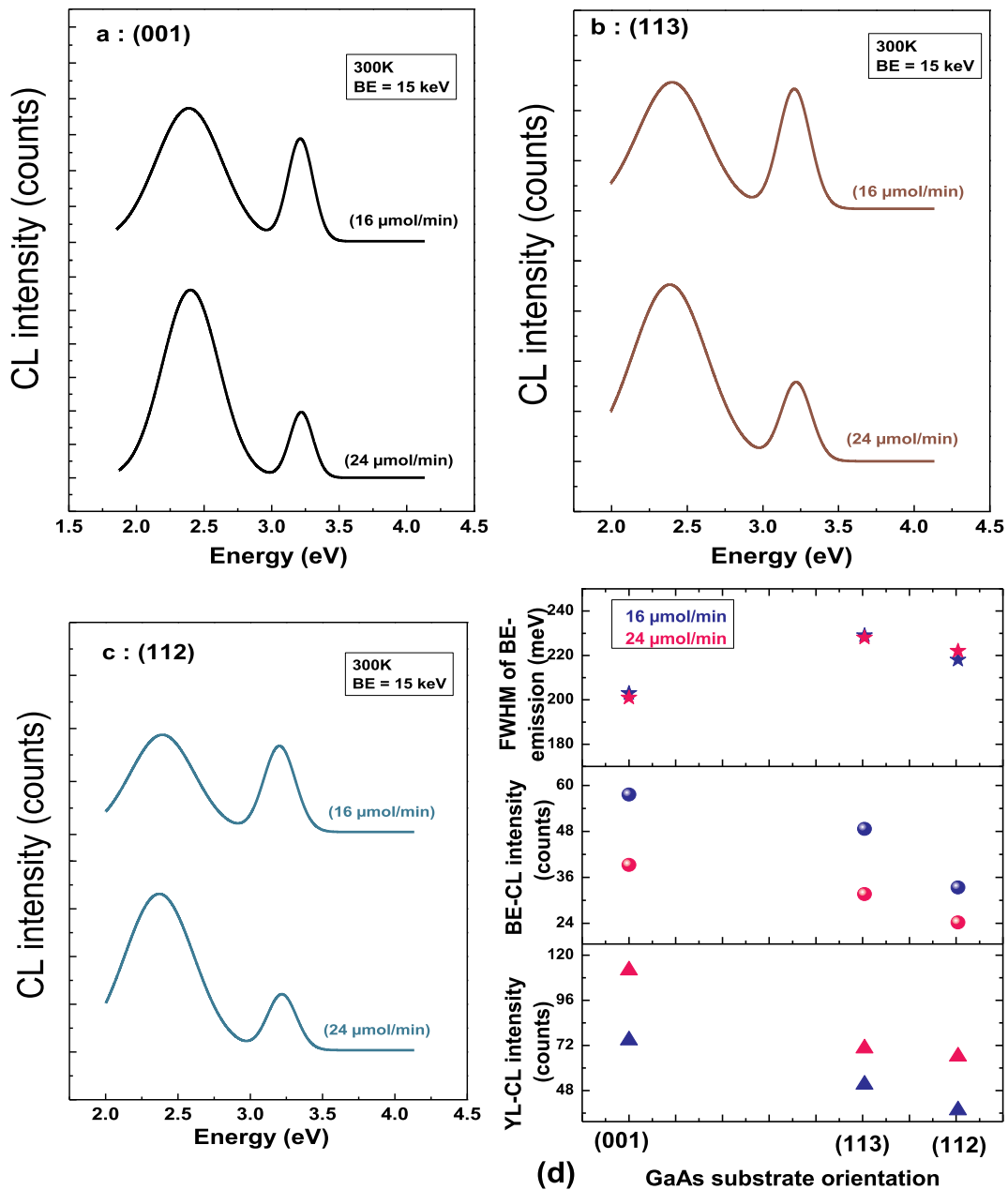
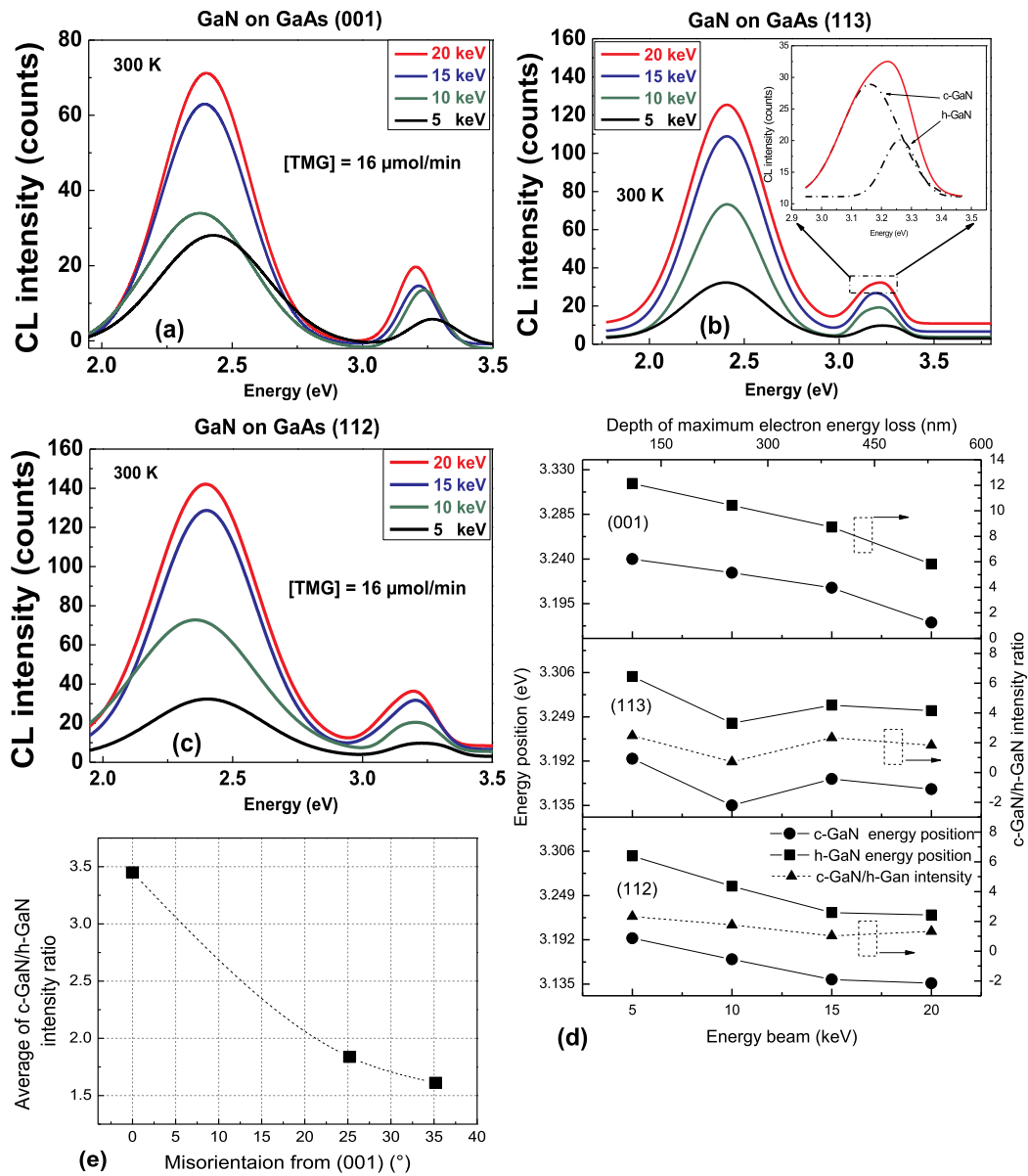


Fig. 6. Cathodoluminescence spectra of GaN layers grown on GaAs (001) (a), (113) (b) and (112) (c) with TMG flow rates of 16  $\mu\text{mol/min}$  and 24  $\mu\text{mol/min}$ . (d) BE-CL intensity, YL-CL intensity and the full width at half maximum of BE-CL emission for all GaN samples.

conditions (thickness of layer and substrate orientation), we plotted the variation of the ratio of c-GaN to the h-GaN intensities as a function of the electron beam energy (as shown in Fig. 7 (d)). This ratio can reflect the fraction of c-GaN crystals in h-GaN layers. It remains almost unchanged as a function of electron beam energy for growth on (113) and (112) GaAs substrates. However, the result obtained for the growth of GaN layers on (001) GaAs substrate shows an increase of the ratio for electron beam energy of 10 and 15 keV which corresponds respectively to 0.2  $\mu\text{m}$  and 0.4  $\mu\text{m}$  of layer thickness, as shown in the upper scale of Fig. 7(d). This result proves that c-GaN fraction is dominant at energy of excitation of 10 and 15 keV. This means that the c-GaN inclusions,

detected by XRD, were localized at the layer thickness range of [0.2–0.4  $\mu\text{m}$ ], as shown in the upper scale of Fig. 7(d).

To conclude, we calculated the average value of the ratio of c-GaN to h-GaN intensities for different electron beam energy values and plotted the result as a function of substrate orientation in Fig. 7 (e). We note that the cubic fraction is dominant with an average value of 3.45 for growth on (001) GaAs substrate compared to the growth on (113) and (112) substrate orientations where the ratio does not exceed the value of 2. Thus, a mechanism of phase transformation occurred by changing the substrate orientations. This is consistent with XRD measurements. The change of c-GaN fraction can be associated with the



**Fig. 7.** (a)-(c) Room temperature CL spectra acquired from the GaN samples grown on (hkl) GaAs substrates with TMG flow rate of 16  $\mu\text{mol}/\text{min}$  at different electron beam energies 5, 10, 15 and 20 keV. The inset in Fig. 7 (b) is a zoom showing the weak shoulder of NBE peak observed for growth of GaN on GaAs (113) at beam energy of 20 keV. (d) NBE peaks position energy variations and  $I_{\text{c-GaN}}/I_{\text{h-GaN}}$  intensity ratio vs. the electron beam energy and the depth of maximum energy loss of GaN layers grown on (001), (113) and (112) GaAs substrates. (e) Average of  $I_{\text{c-GaN}}/I_{\text{h-GaN}}$  intensity ratio as a function of GaAs substrate orientation.

generation of stacking faults (SFs) [16,48]. Indeed, when the SFs were generated in some localized areas the cubic phase turned into a hexagonal one.

#### 4. Conclusion

GaN layers were grown by AP-MOVPE on GaAs (001) and (11n) substrates with TMG flow rate ranging from 16 to 40  $\mu\text{mol}/\text{min}$ . Higher TMG flow rates increased the size and height of the GaN islands due to the excess of Ga migration. For low TMG flow rate, the surface morphology showed an improvement in the RMS and an enhanced coalescence process. CL results showed that reducing TMG flow rate in the GaN layers helps increase the NBE intensity and decrease the YL intensity. For both TMG flow rates of 16 and 24  $\mu\text{mol}/\text{min}$ , all GaN layers grown on the different crystallographic orientations showed the NBE emission of c-GaN. The optimal TMG flow rate of 16  $\mu\text{mol}/\text{min}$  allowed for the growth of GaN on all substrate orientations. Depth resolved-CL

shows that a mechanism of phase transformation occurs by changing the substrate orientation.

#### Acknowledgements

This work is supported by an ARUBE program of DGRST.\*

#### References

- [1] Y. Li, W. Wang, X. Li, L. Huang, Z. Lin, Y. Zheng, X. Chen, G. Li, *J. Alloy. Comp.* 771 (2019) 1000.
- [2] W. Wang, Y. Zheng, X. Zhang, Y. Li, Z. Lu, Guoqiang Li, *Crystal Engineering Community* 20 (2018) 597.
- [3] J.-T. Oh, Y.-T. Moon, J.-H. Jang, J.-H. Eum, Y.-J. Sung, S.Y. Lee, J.-O. Song, T.-Y. Seong, *J. Alloy. Comp.* 732 (2018) 630.
- [4] H. Yang, L.X. Zheng, J.B. Li, X.J. Wang, D.P. Xu, Y.T. Wang, X.W. Hu, P.D. Han, *Appl. Phys. Lett.* 74 (1999) 2498.
- [5] Y.L. Casallas-Moreno, S. Gallardo-Hernández, F. Ruiz-Zepeda, B.M. Monroy, A. Hernández-Hernández, A. Herrera-Gómez, A. Escobosa-Echavarría, G. Santana, A. Ponce, M. López-López, *Appl. Surf. Sci.* 353 (2015) 588.

- [6] H. Vilchis, V.M. Sanchez-R, A. Escobosa, *Thin Solid Films* 520 (2012) 5191.
- [7] D.J. As, *Proc. SPIE* 7608 (2010) 76080G1.
- [8] S. Nakamura, T. Mukai, M. Senoh, N. Iwasa, *Jpn. J. Appl. Phys.* 31 (1992) 139.
- [9] J. Möreke, M.J. Uren, S.V. Novikov, C.T. Foxon, S.H. Vajargah, D.J. Wallis, C.J. Humphreys, S.J. Haigh, A. Al-Khalidi, E. Wasige, I. Thayne, M. Kuball, *J. Appl. Phys.* 116 (2014) 014502.
- [10] S. Strite, J. Ruan, Z. Li, A. Salvador, H. Chen, D.J. Smith, W.J. Choyke, H. Morkoc, *J. Vac. Sci. Technol. B* 9 (1991) 1924.
- [11] R.S. Goldman, R.M. Feenstra, B.G. Briner, M.L. O'Steen, R.J. Hauenstein, *Appl. Phys. Lett.* 69 (1996) 3698.
- [12] J. Laifi, N. Chaaben, H. Bouazizi, N. Fourati, C. Zerrouki, Y. El Gmili, A. Bchetnia, J.P. Salvestrini, B. El Jani, *Superlattice. Microst.* 86 (2015) 472.
- [13] S. Sanorpim, N. Discharoen, K. Onabe, *Phys. Status Solidi C* 7 (2010) 2076.
- [14] T. Makimoto, M. Kasu, J.L. Benchimol, N. Kobayashi, *Jpn. J. Appl. Phys.* 36 (1997) 1733.
- [15] J. Laifi, N. Chaaben, H. Bouazizi, N. Fourati, C. Zerrouki, Y. El Gmili, A. Bchetnia, J.P. Salvestrini, B. El Jani, *Superlattice. Microst.* 94 (2016) 30.
- [16] S. Suandon, S. Sanoprin, K. Yoodee, K. Onabe, *Thin Solid Films* 515 (2007) 4393.
- [17] J. Laifi, N. Chaaben, Y. El Gmili, J.P. Salvestrini, A. Bchetnia, B. El Jani, *Journal of Vacuum* 136 (2017) 8.
- [18] H. Bouazizi, M. Bouzidi, N. Chaaben, Y. El Gmili, J.P. Salvestrini, A. Bchetnia, *Mater. Sci. Eng. B* 227 (2018) 16.
- [19] C. Saidi, N. Chaaben, J. Laifi, T. Sekrafi, O. Tottereau, A. Bchetnia, B. El Jani, *J. Alloy. Comp.* 625 (2015) 271.
- [20] D. Bliss, V. Tassev, D. Weyburne, C. Santeufemio, M. Suscavage, M. Fait, S. Qi Wang, J. Bailey, C. Yapp, R. Kanjolia, J. Anthis, N. Nguyen, L. Smith, R. Odedra, *J. Cryst. Growth* 275 (2005) 1307.
- [21] A. Leycuras, M.G. Lee, *Appl. Phys. Lett.* 65 (1994) 2296.
- [22] B. Beaumont, M. Vaille, T. Boufaden, B. El Jani, P. Gibart, *J. Cryst. Growth* 170 (1997) 316.
- [23] C.-R. Lee, S.-J. Sonn, I.-H. Lee, J.-Y. Leem, S.-K. Noh, *J. Cryst. Growth* 171 (1997) 27.
- [24] Y. Lu, H. Kondo, K. Ishikawa, O. Oda, K. Takeda, M. Sekine, H. Amano, M. Hori, *J. Cryst. Growth* 391 (2014) 97.
- [25] E. Gastellou, C. Morales, G. Garcia, R. Garcia, G.A. Hirata, A.M. Herrera, R. Galeazzi, E. Rosendo, T. Diaz, *Opt. Mater.* 88 (2019) 277.
- [26] M. Konodo, C. Anayama, N. Okada, H. Sekiguchi, K. Domen, *J. Appl. Phys.* 76 (1994) 914.
- [27] M. Wassermeier, J. Sudijono, M.D. Johnson, K.T. Leung, B.G. Orr, L. Daweritz, K. Ploog, *J. Cryst. Growth* 150 (1995) 425.
- [28] S.N. Waheeda, N. Zainal, Z. Hassan, S.V. Novikov, A.A. Akimov, A.J. Kent, *Appl. Surf. Sci.* 317 (2014) 1010.
- [29] M.A. Reshchikova, H. Morkoc, *J. Appl. Phys.* 97 (2005) 061301.
- [30] T. Ogino, M. Aoki, *Jpn. J. Appl. Phys.* 19 (1980) 2395.
- [31] R. Niebuhr, K. Bachem, K. Bombrowski, M. Maier, W. Plerschen, U. Kaufmann, *J. Electron. Mater.* 24 (1995) 1531.
- [32] A.Y. Polyakov, M. Shin, J.A. Freitas, M. Skowronski, D.W. Greve, R.G. Wilson, *J. Appl. Phys.* 80 (1996) 6349.
- [33] R. Zhang, T.F. Kuech, *Appl. Phys. Lett.* 72 (1998) 1611.
- [34] R. Armitage, Q. Yang, H. Feick, S.Y. Tzeng, J. Lim, E.R. Weber, *Mater. Res. Soc. Symp. Proc.* 743 (2003) L10.7.
- [35] S.O. Kucheyev, M. Toth, M.R. Phillips, J.S. Williams, C. Jagadish, G. Li, *J. Appl. Phys.* 91 (2002) 5867.
- [36] E. Silkowski, Y.K. Yeo, R.L. Hengehold, M.A. Khan, T. Lei, K. Evans, C. Cerny, *Mater. Res. Soc. Symp. Proc.* 395 (1996) 813.
- [37] D.C. Oh, S.W. Lee, H. Goto, S.H. Park, I.H. Im, T. Hanada, M.W. Cho, T. Yao, *Appl. Phys. Lett.* 91 (2007) 132112.
- [38] W. Gotz, N.M. Johnson, R.A. Street, H. Amano, I. Akasaki, *Appl. Phys. Lett.* 66 (1995) 1340.
- [39] K. Saarinen, P. Seppala, J. Oila, P. Hautojarvi, C. Corbel, O. Briot, R.L. Aulombard, *Appl. Phys. Lett.* 73 (1998) 3253.
- [40] H. Li, L. Zhang, Y. Shao, Y. Wu, X. Hao, H. Zhang, Y. Dai, Y. Tian, *International Journal of Electrochemical Science* 8 (2013) 4110.
- [41] J. Wu, H. Yaguchi, K. Onabe, R. Ito, *Appl. Phys. Lett.* 71 (1997) 2067.
- [42] A.V. Andrianov, D.E. Lacklison, J.W. Orton, D.J. Dewsnip, S.E. Hooper, C.T. Foxon, *Semicond. Sci. Technol.* 11 (1996) 366.
- [43] K. Knobloch, P. Perlin, J. Krueger, E.R. Weber, C. Kisielowski, *MRS Internet J. Nitride Semicond. Res.* 3 (1998) 4.
- [44] A. Nouiri, S. Chaguetmi, A. Djemel, R.-J. Tarento, *Sci. Technol. Energetic Mater.* 1 (2003) 99.
- [45] A. Hoffman, H. Siegle, A. Kaschner, L. Eckey, C. Thomsen, J. Christen, F. Bertram, M. Schmidt, K. Hiramatsu, S. Kitamura, N. Sawaki, *J. Cryst. Growth* 189/190 (1998) 630.
- [46] Y. El Gmili, G. Orsal, K. Pantzas, T. Moudakir, S. Sundaram, G. Patriarcho, J. Hester, A. Ahaitouf, J.P. Salvestrini, A. Ougazzaden, *Acta Mater.* 61 (2013) 6587.
- [47] L. Liu, J.H. Edgar, *Mater. Sci. Eng. R Rep.* 37 (2002) 61.
- [48] S. Strite, M.E. Lin, H. Morkoc, *Thin Solid Films* 231 (1993) 197.